NUMERICAL STUDIES ON THE ELECTRO-OPTIC SAMPLING OF RELATIVISTIC ELECTRON BUNCHES

S. Casalbuoni, H. Schlarb, B. Schmidt, B. Steffen, DESY, Hamburg, Germany
P. Schmüser, A. Winter, University of Hamburg, Germany

Abstract

Ultraviolet and X ray free electron lasers require sub-picosecond electron bunches of high charge density. Electro-optic sampling (EOS) is a suitable diagnostic tool for resolving the time structure of these ultrashort bunches. The transient electric field of the relativistic bunch induces a polarization anisotropy in a nonlinear crystal which is sampled by femtosecond laser pulses. In this paper, the EOS process is studied in detailed numerical calculations. The THz and the laser pulses are treated as wave packets which are propagated through the zinc telluride resp. gallium phosphide crystals. The effects of signal broadening and distortion are taken into account. The time resolution is severely limited by transverse optical (TO) lattice oscillations (5.3 THz in ZnTe, 11 THz in GaP). The shortest bunch length which can be resolved with moderate distortion is about 200 fs (FWHM) in ZnTe and 100 fs in GaP.

INTRODUCTION

Bunch length measurements in the 100 femtosecond regime are of high interest for VUV and X ray free electron lasers (FEL). The electro-optic sampling (EOS) technique has the potential of eventually reaching this resolution [1]. The principle of the EOS experiment installed at the VUV-FEL [2] is as follows: the electric field co-propagating with the relativistic electron bunch corresponds to short THz pulse that induces a birefringence in an optically active crystal like zinc telluride or gallium phosphide. This optical anisotropy is sampled by an ultrashort polarized laser pulse. In this paper we present the results of numerical studies on the electro-optic effect in zinc telluride (ZnTe) and gallium phosphide (GaP). A detailed presentation can be found in [3].

PROPAGATION OF THE THZ AND LASER PULSES

The best insight into the physics of electro-optic sampling is provided by studying electron bunches and optical laser pulses of Gaussian shape. Other bunch shapes are discussed in [3]. The THz pulse and the optical laser pulse are propagated as wave packets through the EO crystal at their respective group velocities, taking into account pulse broadening and distortion by nonlinear dispersion effects. We use a cylindrical coordinate system ($r = \sqrt{x^2 + y^2}, \theta, z$) with the relativistic beam moving in the z direction. The longitudinal charge distribution in the electron bunch is described by a Gaussian of variance $\sigma_z = c\sigma_t$. The line charge density is then

$\rho(z,t) = \frac{Q}{\sqrt{2\pi}\sigma_z} \exp\left(-\frac{(z-ct)^2}{2\sigma_z^2}\right)$. For highly relativistic electrons the electric field of the bunch has mainly a radial component and can be written as $E_r(r,z,t) = \frac{\rho(z,t)}{2\pi\varepsilon_0 r}$. Let the EO crystal be located at $z = 0$ at a distance r_0 from the beam axis. The electric field at the position of the crystal has the time dependence

$$E_r(t) = \frac{Q}{2\pi\varepsilon_0 r_0 \sqrt{2\pi}c\sigma_t} \exp\left(-\frac{t^2}{2\sigma_t^2}\right). \qquad (1)$$

The Fourier component of the electric field pulse entering the EO crystal is $F_{tr}(f) = F_E(f)\frac{2}{n(f)+i\kappa(f)+1}$, where $F_E(f)$ the Fourier transform of the electric field pulse and $2/(n(f)+i\kappa(f)+1)$ the amplitude transmission coefficient at the vacuum-crystal interface. To propagate the THz pulse inside the EO material we subdivide the crystal into ten thin slices of thickness $\delta = d/10$. The Fourier component at slice j is given by

$$F_{slice\ j}(f) = F_{tr}(f)\exp\left(i\frac{2\pi f}{c}d_j\left(n(f)-i\kappa(f)\right)\right) \qquad (2)$$

where $d_j = (j+0.5)\delta$ is the depth of slice j. The phase propagation is determined by the refractive index $n(f)$, the attenuation by the extinction coefficient $\kappa(f)$. The time profile of the pulse at slice j is then simply obtained by applying the inverse fast Fourier transform to Eq. (2): $E_j^{THz}(t) = IFFT\left[F_{slice\ j}(f)\right]$. To be accurate, also the frequency dependence of the EO coefficient r_{41} must be considered. The "effective" electric THz pulse in slice j is therefore given by

$$E_j^{eff}(t) = IFFT\left[F_{slice\ j}(f) \cdot r_{41}(f)\right] \qquad (3)$$

In the following simulations we have used published data for the refractive index $n(f)$, the extinction coefficient $\kappa(f)$ and the electro-optic coefficient $r_{41}(f)$, collected from the literature quoted in Ref. [3]. These coefficients exhibit resonance-like behavior at the lowest transverse optical (TO) lattice oscillation which is at 5.3 THz in ZnTe and 11 THz in GaP. In Fig. 1 (left) the time profile of a THz pulse of initial variance $\sigma_z = 20$ μm is plotted at selected positions in a 300μm thick ZnTe crystal. The pulse width increases with increasing depth in the crystal and oscillations gradually develop. These high frequency oscillations lag behind the main pulse since the THz refractive index grows approaching the TO resonance of ZnTe at 5.3 THz. Since GaP has a higher TO frequency of 11 THz the 20 μm pulse will propagate in GaP with little distortion. However, a THz pulse of initial variance $\sigma_z = 10$ μm is significantly distorted since it contains Fourier components be-
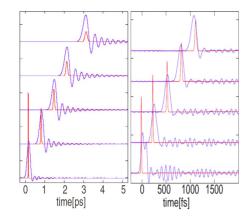
Figure 1: Left: The propagation of a Gaussian THz pulse with initial variance of $\sigma_z = 20\ \mu m$ and of a Gaussian Ti:Sa laser pulse in a 300 μm thick ZnTe crystal. Plotted are the time profiles at selected positions in the crystal. Right: The propagation of a Gaussian THz pulse (variance $\sigma_z = 10\ \mu m$) in a 100 μm thick GaP crystal at selected positions. The frequency dependence of r_{41} is taken into account according to Eq.(3). Shown is also the broadening of a Gaussian Ti:Sa laser pulse.

yond 11 THz. In Fig. 1 (right) the propagation of such a narrow THz pulse in a 100 μm thick GaP crystal is shown. The Ti:Sa laser pulse changes also its shape because the optical refractive index has a nonlinear dependence on the wavelength. Assuming a Gaussian distribution for the laser intensity $I_{las}(t) \propto \exp\left(-\frac{t^2}{2\sigma_0^2}\right)$ with a bandwidth-limited FWHM (full width at half maximum) of $\Delta t = 2\sqrt{2\ln 2}\sigma_0 = 15$ fs for the Ti:Sa laser (Femtosource COMPACT, Femtolasers, Vienna) used in our EOS experiment we expect a growth of the variance with increasing depth in the EO crystal [4] $\sigma(z) = \sigma_0 \sqrt{1 + \left(\frac{z}{L_{char}}\right)^2}$ with a characteristic length $L_{char} = \Delta t^2 / (4\ln 2 \frac{d}{d\omega}(v_g^{-1}))$. One gets $L_{char} = 30\ \mu m$ in ZnTe and $L_{char} = 42\ \mu m$ in GaP. Figure 1 shows the THz and laser pulses at selected positions inside the 300 μm thick ZnTe crystal and the 100 μm thick GaP crystal. The laser pulse moves at a lower speed than the THz pulse, and due to the nonlinear dispersion its width increases.

Electro-optic signal

The highest EO sensitivity is obtained when the angle between the electric vector of the THz field and the crystallographic axis [-1,1,0] is chosen as $\alpha = 0$. The main axes of the refractive index ellipse are then oriented at $\alpha = 45°$ resp. $\alpha = 135°$. The laser is linearly polarized, with the electric vector parallel to the [-1,1,0] axis. Its two orthogonal projections on the long resp. short half axis of the refractive index ellipse receive a relative phase shift in the birefringent crystal. This is called the phase retardation parameter Γ. Approximating the laser pulse

by a delta function we see immediately from the above figures that the retardation parameter Γ_j [3], generated in slice j, is proportional to the (effective) electric field amplitude $E_j^{eff}(t_{j,laser})$ at the arrival time of the laser pulse in slice j, $\Gamma_j = \frac{2\pi}{\lambda_0}n_0^3 \delta\, E_j^{eff}(t_{j,laser})$. This time is $t_{j,laser} = d_j/v_{group} + \tau$ where we have allowed for a variable time delay τ between THz and laser pulse. The total phase retardation accumulated in the EO crystal can be computed as a sum over the contributions of each slice:

$$\Gamma(\tau) = \sum_j \Gamma_j(\tau) = \frac{2\pi}{\lambda_0}n_0^3 \delta \sum_j E_j^{eff}\left(d_j/v_{group} + \tau\right) .$$

(4)

In the actual EOS experiment the delay τ is varied in small steps to scan the THz pulse. The two orthogonal laser pulse components are spatially separated by means of a $\lambda/4$ plate and a Wollaston prism and then guided to the two diodes of a balanced detector. It can be shown [5] that the balanced detector signal is proportional to $\sin(\Gamma)$.

The next refinement would be to incorporate the finite laser pulse width and broadening. This is discussed in Ref. [3]. It turns out that the influence of laser pulse broadening is only visible in a rather thick EO crystal and insignificant for most practical cases.

QUALITY OF BUNCH SHAPE DETERMINATION BY EOS

Here we summarize the simulation results for ZnTe and GaP crystals for THz pulses of various width. The bunch charge is chosen as $Q = 0.5$ nC, the distance between the electron beam and the spot on the EO crystal which is scanned by the laser is taken as $r_0 = 14$ mm. We consider a GaP crystal of 100 μm thickness. The balanced detector signal expected from a pulse with $\sigma_z = 20\ \mu m$ is shown in Fig. 2a. The original pulse shape is almost reproduced, only the width increases by 15%. Note that no oscillations are observed in the tail of the detector signal. This is easily understood since the 20 μm bunch has very small Fourier components near the TO resonance of GaP at 11 GHz. A shorter bunch, however, leads to oscillations in the detector signal, and a significant pulse stretching (the FWHM is a factor 1.6 wider), see Fig. 2b.

In Fig. 3a we show the broadening factor as a function of the rms bunch length for ZnTe and GaP. Above 30 μm both EO materials are suited to reconstruct the shape without distortion. It is evident that GaP permits the measurements of far shorter pulses than ZnTe. However, bunch lengths with $\sigma_z \le 10\ \mu m$ cannot be resolved even with a GaP EO crystal. The FWHM of the EO signal is plotted in Fig. 3b as a function of the FWHM of the incoming pulse. It is evident that the lowest measurable FWHM is 200 fs in ZnTe and 100 fs in GaP. Note that we have neglected here any time jitter between the THz and laser pulses.

Ideally the amplitude of the EO signal should be directly proportional to the thickness d of the EO crystal. In reality, the THz pulse distortion leads to a slower than linear rise
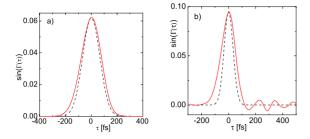
Figure 2: GaP crystal, $d = 100~\mu m$. a) The balanced-detector signal (solid curve) of a ($\sigma_z = 20~\mu m$) THz pulse in comparison with the original pulse shape (dashed curve). b) The balanced-detector signal (solid curve) of a shorter THz pulse ($\sigma_z = 10~\mu m$) compared to the original pulse shape (dashed curve).
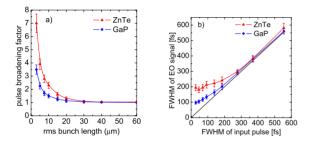

Figure 3: Pulse broadening in ZnTe (triangles) and in GaP (circles). The EO crystal has a thickness $100~\mu m$. a) Pulse broadening factor as a function of the initial rms bunch length.
b) FWHM of the EO signal as a function of the FWHM of the electron bunch.

of the balanced detector signal with d and eventually to a saturation. This is demonstrated in Fig. 4. Another disadvantage is that the FWHM of the signal grows considerably towards larger thickness. In order to preserve a good time resolution the crystal thickness should therefore not exceed $d = 100~\mu m$ by a large factor. On the other hand, going to $d = 50~\mu m$ or less does not really improve the resolution but only leads to much smaller signals.

CONCLUSIONS

Using the available experimental data on the material properties of ZnTe and GaP (frequency-depenent complex refractive index and electro-optic coefficient) we have studied the effects of pulse broadening, pulse shape distortion and group velocity mismatch in EOS experiments. Only the standard case has been considered where both the THz and the femtosecond laser pulse impinge perpendicular to the surface of the EO crystal. Our conclusion is that the shortest pulse length which can be recovered without significant distortion amounts to 200 fs (FWHM) in ZnTe and to 100 fs in GaP. The main limitation for the shortest time
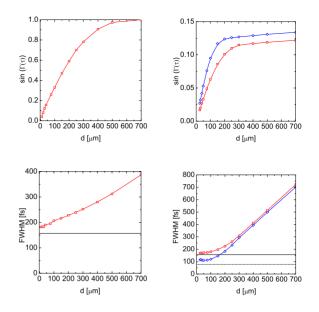

Figure 4: Dependence of the electro-optic signal on the thickness d of the EO crystal. Top graphs: signal amplitude $\sin(\Gamma)$ vs. the thickness d. Left: a pulse with $\sigma_z = 20~\mu m$ in ZnTe; right: a pulse with $\sigma_z = 20~\mu m$ (squares) and with $\sigma_z = 10~\mu m$ (diamonds) pulse in GaP. Bottom graphs: FWHM of the detector signal as a function of d. Left: ZnTe, right: GaP. The FWHM of the incident pulse is shown as a solid line ($\sigma_z = 20~\mu m$) and as a dashed line ($\sigma_z = 10~\mu m$).

structure which can be resolved is given by transverse optical (TO) lattice oscillations. The lowest TO frequency amounts to 5.3 THz for ZnTe and 11 THz for GaP. Near a resonance the refractive index is rapidly changing and it is basically impossible to achieve equal group velocities of the THz and the laser pulse. Obviously, GaP is better suited to measure very short pulses owing to its higher TO frequency. The disadvantage is that the electro-optic coefficient of GaP is a factor of eight lower than that of ZnTe. In this paper we have not considered more advanced EO techniques such as temporal decoding [1] which permit single-shot electron bunch diagnostics. However, the limitations on time resolution that are caused by the TO resonances are also present in these techniques.

REFERENCES

[1] G. Berden et al., Phys. Rev. Lett. **93** 114802 (2004).

[2] B. Steffen et al., this proceedings.

[3] S. Casalbuoni et al., TESLA Report 2005-01, http://tesla.desy.de/new_pages/TESLA_Reports/2005/ pdf_files/tesla2005-01.pdf.

[4] D. Meschede, Optics, Light and Lasers, WILEY-VCH-Verlag, 2004 Weinheim.

[5] M. Brunken et al., TESLA Report 2003-11.